Indian Journal of Pure & Applied Physics
Vol. 57, September 2019, pp. 684-689

Study of clustering, pairing and resonances in direct nuclear reactions

Arun K Jain* & B N Joshi

Nuclear Physics Division, Bhabha Atomic Research Center, Mumbai 400 085, India

Received 3 July 2019

At energies from about 10 MeV to 100's of MeV the light incident projectiles incident on medium heavy targets produce nuclear reactions which normally come under the category of direct reactions. At such energies one can study the microscopic structure of nuclei because the wave length is comparable to the inter nucleon separations in nuclei. Besides the normal independent particle behavior one can study the influences of the short range and long range residual interactions in the form of pairing and clustering in nuclei. The resonances existing as the molecular nuclear structures comprising of ^{12}C-^{12}C and ^{16}O-^{8}Be structure in ^{24}Mg* has given rise to interesting phenomenon of perturbing resonances in heavy cluster knockout reactions.

Keywords: Clustering, Pairing, Resonances, Direct reactions

1 Introduction

It has been known for several decades that the single particle behavior of nuclei is governed by the mean field experienced by the nucleons from the adjoining nucleons as a result of the short range nature of the nucleon-nucleon (n-n) interaction. The microscopic behavior of nuclei in terms of independent particle shell model has been verified by the direct reactions of the type of (p, d), (d, ^{3}He) and (p, 2p) etc. at few tens to few hundreds of MeV. Besides the dominant single particle behavior of nucleons in nuclei the nucleons also experience the short and long range residual interactions which remove the single particle degeneracy of the various low lying single particle nuclear levels. The two body residual n-n interactions lead to two body correlations which give rise to clustering in the surface regions of nuclei and pairing of nucleons in the interior of nuclei.

To study the clustering aspect, the cluster knockout reactions had been the best bet, but due to the demand of huge computational power, for a proper distorted wave calculation, simplifications of the type of zero-range, eikonal and plane wave approximations were taken resort to. These resulted in uncertainties which prevented any predictive power to the knockout reactions. In the last decade we have been able to circumvent some of these uncertainties with the inclusion of finite range aspects associated with the transition matrix element of the knockout vertex. This has resulted in an unexpected gain, in that one could recover the predictive power of the knockout reactions. It has also shattered some of the myths associated with the effective interactions used in the form of M3Y interactions[1,2] and various other types of Love-Franey effective n-n interactions[3,4]. One of the common drawbacks of these interactions is that they were based on the perturbation theory, where the solution of the Schrodinger equation incorporating the realistic n-n interaction does not appear at all. One of the outcomes of the effective interactions derived from the solution of the Schrodinger equation is that the derived effective interaction[5] vanishes at small separations as opposed to the M3Y and the Love-Franey interactions which peak at small separations. Besides this, the operators such as spin-orbit or tensor operators appearing in the Love-Franey effective interactions disappear in our formalism due to their operations on the distorted wave functions. This procedure, with partial wave expansion of the wave function, leads to effective interactions as expansion in legendre polynomials which can be used in the evaluation of the optical potentials using the double folding procedure as well as for the transition operators in the knockout reactions.

2 Theoretical Formulation

The transition amplitude, T_{fi} for the knockout reaction A (a,ax)B in the FR-DWIA formalism from the initial state[6–8], *i* to the final state, *f* can be written as:

$$\frac{d^3\sigma^{L,J}}{d\Omega_1 d\Omega_2 dE_1} = F_{kin} \cdot S_x^{LJ} \cdot \sum_{\Lambda} | T_{fi}^{xL\Lambda}(\vec{k}_f, \vec{k}_i) |^2, \quad \ldots (1)$$

*Corresponding author (E-mail: arunjain@barc.gov.in)

Where, J and L (∧) are the total and orbital (its azimuthal component) angular momenta of the bound x-particle in the target nucleus, F_{kin} is a kinematic factor and S_x^{LJ} is the cluster spectroscopic factor. The conventional transition matrix element for the knockout reaction, $T_{fi}^{xL\Lambda}(\vec{k}_f,\vec{k}_i)$ using the finite range α-x t-matrix effective interaction[6–8] t_{12} (r_{12}) is given by:

$$T_{fi}^{xL\Lambda}(\vec{k}_f,\vec{k}_i)=\int \chi_1^{(-)*}(\vec{k}_{1B},\vec{r}_{1B})\chi_1^{(-)*}(\vec{k}_{2B},\vec{r}_{2B})$$
$$t_{12}(\vec{r}_{12})\chi_0^{(+)}(\vec{k}_{1A},\vec{r}_{1A})\varphi_{L\Lambda}(\vec{R}_{2B})d\vec{r}_{12}d\vec{R}_{2B}. \quad \ldots (2)$$

Here, the $t_{12}(\vec{r}_{12})$, evaluated at the final state relative energy[5] E_f, is given by:

$$t_{12}^{+}(E,\vec{r})=e^{-ikz}V(\vec{r})\Psi_{12}^{+}(\vec{r})\equiv\sum_{L=0,1,2,\ldots.}t_L(E,r)P_L(\hat{r}). \quad \ldots (3)$$

Where,

$$\Psi_{12}^{+}(\vec{r})=\sum_{\ell=0,2,4,\ldots}i^{\ell}(2\ell+1)\frac{u_\ell(kr)}{kr}e^{i\sigma^{\ell}}P_\ell(\hat{r}) \quad \ldots (4)$$

As discussed in literature[5] the L_{th} multiple of the $t_{\alpha\alpha}^{+}(E,\vec{r})$ can be written:

$$t_L(E,r)=\frac{2L+1}{2}\sum_{\ell,n}V_\ell(r)i^{\ell}(2\ell+1)\frac{u_\ell(kr)}{kr}J_n(kr)$$
$$(-i)^n(2n+1)e^{i\sigma^{\ell}}\int_{-1}^{+1}P_L^{*}(\cos\theta)P_\ell(\cos\theta)$$
$$P_n(\cos\theta)d(\cos\theta) \quad \ldots (5)$$

The distorted waves χ_0, χ_1 and χ_2 of Eq. (2) are evaluated for the α1-A, α1-B and x-B optical potentials. Finally all the relative coordinates are expressed in terms of $\vec{r}_{12}(\equiv\vec{r})$ and $\vec{R}_{2B}(\equiv\vec{R})$. While using the PWIA the transition matrix element, T_{fi} of Eq. (2) was factorized into integrals over $\vec{r}$ and $\vec{R}$, separately. The same is not possible when one uses the full finite range t_{12} ($\vec{r}_{12}$) due to the presence of optical distortions. This is because in the FR-DWIA formalism the chosen relative coordinates $\vec{r}$ and $\vec{R}$ get coupled through the distorted waves $\chi_0^{(+)}(\vec{k}_{1A},\vec{r}_{1A})$ and $\chi_0^{(+)}(\vec{k}_{1B},\vec{r}_{1B})$.

For the evaluation of $T_{ft}^{xL\Lambda}$ of Eq. (2) the distorted waves, $\chi(\vec{k},\vec{r})$ were expanded in terms of partial waves and then on the mesh of the spherical polar coordinates, r, θ, φ and R, Θ, Φ the values of χ_0, χ_1, χ_2, φL($\vec{R}$) and $t_{12}(\vec{r})$ were evaluated. The final result of T_{fi} is obtained by doing a 6-dimensional integration over the mesh of $\vec{r}$ and $\vec{R}$ coordinates. The computer code was checked by performing FR-plane wave impulse approximation (PWIA) calculations using the present 6-dimensional integration approach as well as through the 3-dimensional integrations approach (because in the plane wave case the 6-dimensional integral of Eq. (2) factorizes into two separate 3-dimensional integrals, over $\vec{r}$ and $\vec{R}$, respectively.

3 Results and Discussion

Using the zero-range (ZR) distorted wave impulse approximation (DWIA) for cluster knockout reactions the predicted cross sections were orders of magnitude too small resulting in huge and absurd spectroscopic factors[6,9–12]. On the other hand when finite range-(FR)-DWIA calculations were performed, using the finite range effective inter actions derived from the realistic interactions which reproduce the corresponding elastic scattering data, then one could get very good predictions (see Figs. 1 and 2) for the

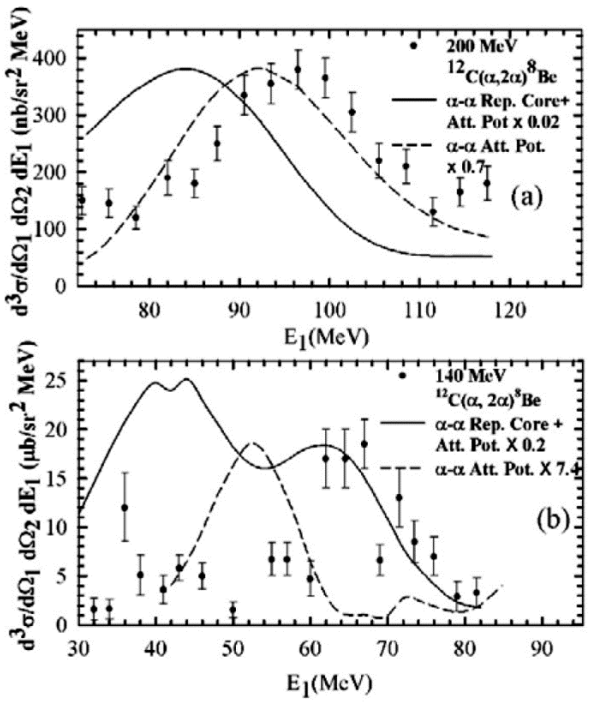

Fig. 1 – Comparison of ^{12}C (α, 2α) energy sharing data with the FR-DWIA calculations using α-α interaction which is, purely attractive (A) and having a repulsive core (R+A), (a) for 200 MeV and (b) for 140 MeV.

absolute cross sections[13] (see Table 1). In Table 1 it is seen that the absolute cross sections and S_α values for the ~197 – 200 MeV (α, 2α) reactions on ^{9}Be and ^{12}C using the purely attractive $t_{\alpha\alpha(A)}(\vec{r}\,)$ are in better agreement with data in comparison to that using $t_{\alpha\alpha(R+A)}(\vec{r}\,)$ where the absolute cross sections are about an order of magnitude too large. For energies at and below ~140 MeV, both the $t_{\alpha\alpha(A)}(\vec{r}\,)$ and $t_{\alpha\alpha(R+A)}(\vec{r}\,)$ yield somewhat distorted shapes. Yet the peaks close to the zero recoil momentum position (normalized to the data peak values) yield S_α-values, seen in Table 1, much closer to the theoretical values when $t_{\alpha\alpha(R+A)}(\vec{r}\,)$'s are employed. On the other hand, the S_α-values obtained from the $t_{\alpha\alpha(A)}(\vec{r}\,)$'s are more than an order of magnitude too large as compared to theory.

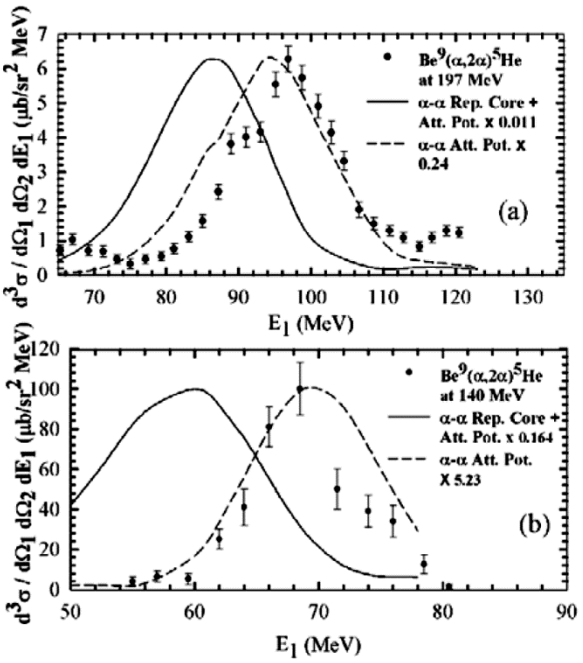

Fig. 2 – Comparison of ^{9}Be (α, 2α) energy sharing data with the FR-DWIA calculations using α-α interaction which is purely attractive (A) and having a repulsive core (R+A), (a) for 197 MeV and (b) for 140 MeV.

Differences of orders of magnitude are seen between the FR-DWIA predictions of the (α, 2α) reaction cross sections using the repulsive core, (R+A) and purely attractive, (A) α-α potentials. An obvious conclusion is that use of the conventional ZR-DWIA formalism and hence the factorization approximation for the analysis of (α, 2α) reactions below ~197 MeV was improper. From these FR-DWIA results it is obvious that the α-α potential character changes drastically at α-energies, E_α somewhere between 140 and 200 MeV, corresponding to the centre of mass energy $E_{\alpha\text{-}\alpha}$ of 70-100 MeV. Again this can be qualitatively understood in the resonating group method, (RGM)-shell model picture (which takes care of the Pauli's exclusion principle). Here the four neutrons (n) and four protons (p) of the two α-particles can exist in an overlapping position if the two n's and two p's of one α-particle are in the lowest $1s_{1/2}$ shell model state and the other two n's and two p's of the other α-particle in the next shell model state ($1p_{3/2}$, which is situated around 21 MeV above the ground state of the α-particle). The total energy of this overlapping system, $E_{\alpha\text{-}\alpha}$ will thus be ~4×21 MeV= 84 MeV (corresponding to E_α ~2×84=168 MeV). Thus below this energy, E_α ~168 MeV, the two α's would find it energetically more favorable to avoid their overlap with a repulsive core in their interaction. Above this energy, however the two α's have no such restriction and are free to have the usual attractive force between them. This understanding of the change in the nature of the α-α interaction is clearly validated by the present FR-DWIA analyses of the (α, 2α) energy sharing data.

The α-knockout and ^{12}C-knockout should give rise to similar spectroscopic factor for the α-^{12}C structure of ^{16}O-nucleus. Comparative results for the FR-DWIA analysis of 140 MeV ^{16}O (α, 2α)^{12}C and the 120 MeV ^{16}O(^{12}C, 2^{12}C)^{4}He reaction (seen in Fig. 3)[13,14] prove the validity of heavy cluster knockout mechanism also. The FR-DWIA analysis of this reaction indicated that even the ^{12}C-^{12}C interaction has a repulsive core around ~ 60 MeV cm energy.

Table 1 – Comparison of (α, 2α) cross sections from FR-DWIA calculations and experimental data on ^{9}Be and ^{12}C at various energies and spectroscopic factors (Sα) derived from the FR-DWIA calculations and theory. Comparison of bold face entries is emphasized for their reasonableness.

Reaction	Eα	σα, 2α (Peak) μb/sr2 MeV			Sα		
	(MeV)	(R+A)	(A)	Expt	(R+A)	(A)	Theory
^{9}Be(α, 2α)^{5}He	197	575	26.4	6.3	0.011	0.24	0.57
	140	609	19.1	100	0.164	5.23	
^{12}C(α, 2α)^{8}Be	200	19.9	0.552	0.380	0.02	0.7	0.55, 0.29
	140	92	2.5	18.5	0.2	7.4	

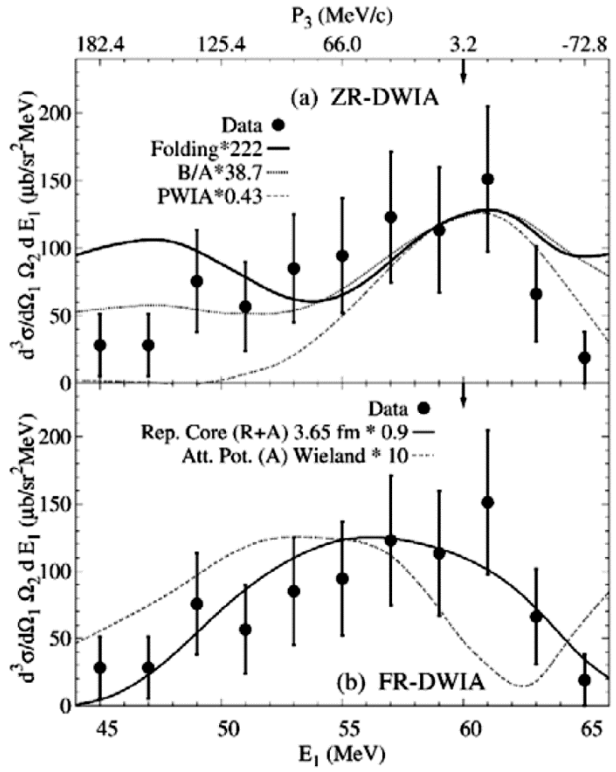

Fig. 3 – Energy sharing spectrum for 119 MeV $^{16}O(^{12}C, 2^{12}C)^{4}He$ fitted with (a) ZR-DWIA and (b) FR-DWIA results using ^{12}C-^{12}C potential, purely attractive (A)-dashed line, and having a repulsive core (R + A). The spectroscopic factors are indicated in the legend.

In the excited state of ^{24}Mg there are large number of resonances[16] which exist upto an excitation energy of ~56MeV and angular momentum of upto $22\hbar$. In an experiment at 104 MeV $^{24}Mg(^{12}C, 2^{12}C)^{12}C$ reaction[17] the kinematics was chosen such that in the 3-body final state, there are two 2-body resonances in the relative motions of the two ^{12}C's in the two arms of the three ^{12}C forming a triangle. In this kinematics the energies and angles were chosen such that the two 38.5 MeV 18^{+} ^{24}Mg*-resonances overlap at an energy of E_1=45 MeV and E_2=45 MeV of the two outgoing detected ^{12}C's, see Fig.4. It was found that at this position the coincidence cross section almost vanishes. This is an interesting observation because from this one can infer that the direct knockout of ^{12}C from the ^{12}C-^{12}C component in the ground state of ^{24}Mg is negligible. Moreover the vanishing resonance contribution also indicates that in any reaction where the resonance is merged with the background one can find a dip in the cross section when the same resonance is produced in a three-body reaction with the two resonances overlapping at some kinematic point. This is because at the dip position only the non-

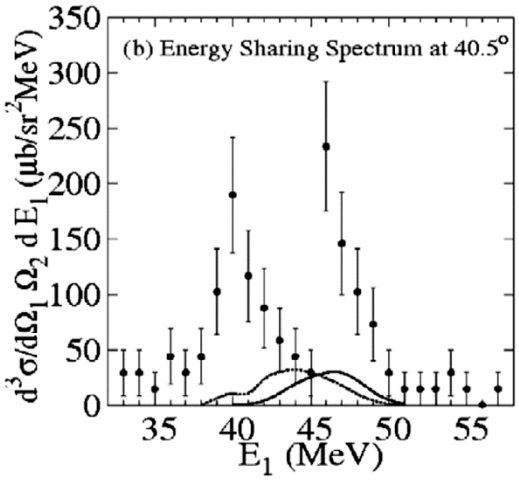

Fig. 4 – Results for 104 MeV 24 Mg (^{12}C, $2^{12}C)^{12}C$ reaction at θ1=θ2=40.50. The two detected ^{12}C's have relative motions with respect to the residual ^{12}C corresponding to 18+36.5 MeV excited state of ^{24}Mg each when E1=E2=45 MeV.

resonant cross section will survive. Besides this the whole concept of the two 2-body resonances in a 3-body system perturbing each other destructively can be utilized in many areas such as in the production of σ-meson as a resonance perturbation in a π-N-π system where the two π-N systems form Δ resonance each, giving rise to a characteristic mass and width of the σ-meson. This phenomenon is similar to the one producing the dark rings of the planet Saturn by the perturbation caused by its moon, the Titan, on the particle (which existed in its orbit in the dark band if the Titan was not existing) to move it to an adjacent orbit.

For the existence of clusters one looks beyond the independent particle shell model where one finds that nucleons correlate in the low density surface region of the nucleus due to the long range residual interaction. For example in ^{6}Li the two neutrons and two protons in the $1s_{1/2}$-shell form an α-cluster while the one neutron and one proton in the $1p_{3/2}$-shell correlate to form a deuteron cluster due to this all of them are effectively forming the low density surface of the independent particle shell model nucleus. It has been seen in the ^{6}Li (d, tp) ^{4}He reaction[15] that this reaction behaves more like a d(d, t)p reaction where the α-particle is behaving as a spectator. It has been demonstrated in this experiment that on an average when the α-cluster is far away from the deuteron cluster in ^{6}Li-nucleus then it is more or less similar to the free deuteron but when it moves closer to the α-cluster then it shrinks to a smaller size. This shrinkage is the result of the individual nucleons in

the $1p_{3/2}$-shell forming the deuteron cluster interact with the α-cluster as also due to the long range residual interaction (a remnant of the n-n interaction after removing the single particle shell model potential).

Although the influence of the long range residual interaction is witnessed in this study of ^{6}Li(d, tp)^{4}He reaction a similar study for the short range residual interaction has not been forthcoming. However, in the analysis of (p, d) reactions at around 700 to 800 MeV[18,19,21,22] some helplessness is felt while analyzing these (p, d) reaction data. The situation is worst with the analysis of 770 MeV ^{4}He (p, d) ^{3}He reaction[20]. The plane wave (PW) as well as the distorted wave born approximation (DWBA) analysis[19–22] of this data shows a much sharper angular distributions than what the data indicated. Varying distorting potentials as well as incorporating correlations of the Jastrow type did not result in any significant improvement[20]. In order to understand this data the problem was addressed from the point of view of incorporating the short range n-n-residual pairing interaction in the wave function of the bound neutron which is picked up by the incoming proton. We started with the microscopic 4-nucleon shell model harmonic oscillator wave function for ^{4}He and then using Brody-Moshinsky transformation[23] expressed this wave function as a function of the relative coordinates of the two protons and the two neutrons along with their centre of mass motion wave functions. Now the relative n-n wave function should in fact be the solution of the Schrodinger equation incorporating the n-n short range residual (pairing) interaction beside some longer range single particle model interaction. Therefore for the n-n radial wave function we solved a bound state Schrodinger equation incorporating a Woods Saxon potential along with the v_{14} Argonne n-n interaction[24] for the neutron-neutron (n-n) as well as proton-proton (p-p) T =1, S=0 and L=0 states. Solutions of these paired n-n and p-p relative motions are then replaced by these solutions of the Schrodinger equations in place of the shell model relative wave functions. Next we used the Fourier Transform techniques to correct for the fictitious c.m. motion.

Now the plane wave born approximation transition matrix element for the ^{4}He(p, d)^{3}He reaction can be immediately written as a product of the Fourier transform of the deuteron wave function and another Fourier transform of the n-^{3}He wave function. Here we have used the same first integral DL(Δ) as in literautre[19] which uses the Reid soft core interaction[25] and where the L=2, d-state contribution is dominant. For the $\Phi_{n\tau}$ ($r_{n\tau}$) we used the above mentioned procedure which produces the s-state wave function using the Argonne V_{14} -interaction[24] for the short range part along with a longer range Woods Saxon potential. This wave function is presented in Fig. 5. The Fourier transform of this wave function is used for the calculation of the angular distribution (seen in Fig. 6) using these ingredients. Now one can see that

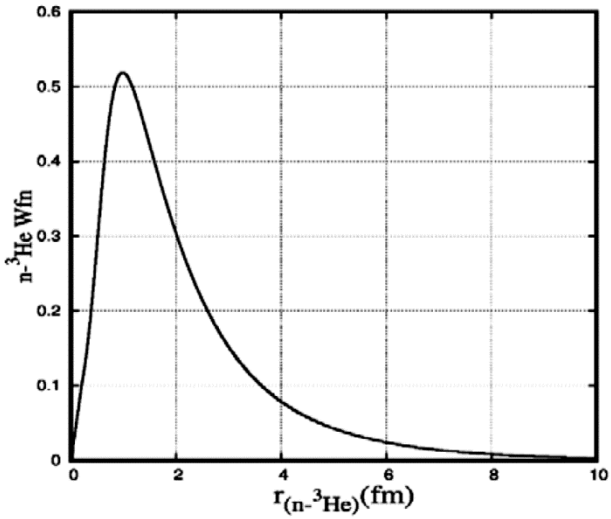

Fig. 5 – n-^{3}He wave function component of ^{4}He-nucleus incorporating the n-n correlations obtained from the solution of the Schrodinger equation incorporating the v14 Argonne n-n interaction[24] along with a Saxon-Woods potential. The c.m. motion correction is included in this evaluation.

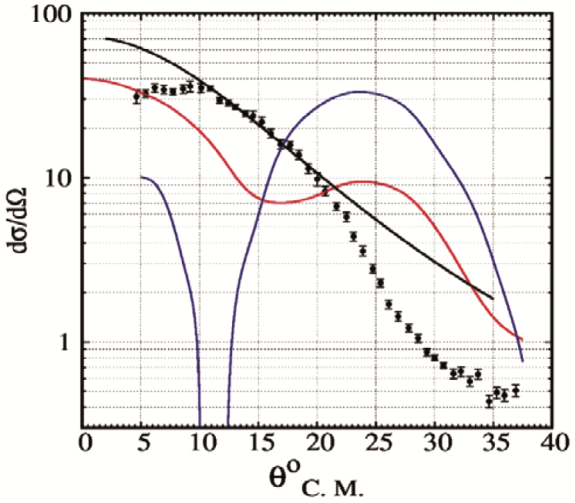

Fig. 6 – 770 MeV ^{4}He(p, d)^{3}He reaction, P.W. calculations (black line) using short range n-n correlating interaction compared with the results of Rost *et al*. blue line (PWBA) and red line (DWBA).

while there are huge differences between the PW and DWBA calculations of Rost *et al.*[20] with the data because there are too few large momentum components in their wave functions, $\Phi_{n\tau}$ ($r_{n\tau}$) as compared to enhanced large momentum components present in our n-τ -wave function. It is seen that our PW calculations fit the data much better except for some differences at small angles and similar small difference at large angles. These differences probably can be understood in terms of a proper evaluation of the DL(Δ) term which in the present work we used only a simplified perturbative evaluation by Rost and Shepard[19] using Reid Soft core potential[25] for the deuteron. One can easily witness in Fig. 6 that these short range residual interactions produce a large dent in $\Phi_{n\tau\ (r n\tau\ )}$ around $r < 1_{fm}$ it is to be noted that these calculations can be improved using proper distorted wave functions incorporating the n-n interactions in the wave functions of the deuteron itself. Thus, avoiding the Born approximation altogether, which will correspond to the incorporation of the triplet S = 1-state interaction containing the D-state through the large contribution from the Tensor interaction directly. Here it can be stated that the large momentum components in the nuclear single particle wave functions are naturally introduced by the short range n-n interaction which effectively represents the n-n-pairing interaction and produces a dent at the central density of the ^{4}He nucleus.

4 Conclusions

In conclusion it can be said that the single particle picture is a very simplified model. For the understanding of the high precision and novel experiments one requires the incorporation of the clustering, pairing and resonance perturbation phenomena in the theoretical frameworks as also more computational power for better predictability in nuclear physics.

Acknowledgement

AKJ thanks Bhabha Atomic Research Centre, Mumbai for providing the necessary infrastructure support. This work is financially supported by the SERB of the Department of Science and Technology, Govt of India.

References

1 Bertsch G, Borysowicz J, McManus H & Love W G, *Nucl Phys A*, 284 (1977) 399.
2 Satchler G R & Love W G, *Phys Rep*, 55 (1979) 183.
3 Love W G & Franey M A, *Phys Rev C*, 24 (1981) 1073.
4 Franey M A & Love W G, *Phys Rev C*, 31 (1985) 488.
5 Jain A K & Joshi B N, *Prog Theor Phys*, 120 (2008) 1193.
6 Chant N S & Roos P G, *Phys Rev C*, 15 (1977) 57.
7 Jacob G & Maris T A J, *Rev Mod Phys*, 38 (1966) 121.
8 Jackson D F & Berggren T, *Nucl Phys*, 62 (1965) 353.
9 Wang C W, Chant N S, Roos P G, Nadasen A & Carey T A, *Phys Rev C*, 21 (1980) 1705.
10 Carrey T A, Roos P G, Chant N S, Nadasen A & Chen H L, *Phys Rev C*, 23 (1981) 576.
11 Cowley A A, Steyn G F, Förtsch S V, Lawrie J J, Pilcher J V, Smit F D & Whittal D M, *Phys Rev C*, 50 (1994) 2449.
12 Steyn G F, Förtsch S V, Cowley A A, Lawrie J J, Arendse G J, Hillhouse G C, Pilcher J V, Smit F D & Neveling R, *Phys Rev C*, 59 (1999) 2097.
13 Jain A K & Joshi B N, *Phys Rev Lett*, 103 (2009) 132503.
14 Joshi B N, Jain A K, Gupta Y K, Biswas D C, Saxena A, John B V, Danu L S, Vind R P & ChoudhuryR K, *Phys Rev Lett*, 106 (2011) 022501.
15 Grossiord J Y, Coste C, Guichard A, Gusakow M, Jain A K, Pizzi J R, Bagieu G & Swiniarski R de, *Phys Rev Lett*, 32 (1974) 173.
16 Freer M, *Rep Prog Phys*, 70 (2007) 2149.
17 Joshi B N, Jain A K, Biswas D C, John B V, Gupta Y K, Danu L S, Vind R P, Prajapati G K, Mukhopadhyay S & Saxena A, *PRAMANA*, 88 (2017) 29.
18 Bauer T, Boudard A, Catz H, Chaumeaux A, Couvert P, Garçon M, Guyot J, Legrand D, LugoL J C, Matoba M, Mayer B, Tabet J P & Terrien Y, *Phys Lett B*, 67 (1977) 265.
19 Rost E & Shepard J R, *Phys Lett B*, 59 (1975) 413.
20 Rost E, Shepard J R & Sparrow D A, *Phys Rev C*, 17 (1978) 1513.
21 Jain B K, *Phys Rev C*, 27 (1983) 794.
22 Smith G R, Shepard J R, Boudrie R L, Peterson R J, Adams G S, Bauer T S, G J Igo, Pauletta G, Whitten C A Jr, Wriekat A, Hoistad B & Hoffmann G W, *Phys Rev C*, 30 (1984) 593.
23 Moshinsky M, *Cargese Lectures Phys*, 3 (1974).
24 Wiringa R B, Stoks V G J & Schiavilla R, *Phys Rev C*, 51 (1995) 38. Reid R V, *Ann Phys*, 50 (1968) 411.